Journal of Materials Science: Materials in Engineering

ORIGINAL PAPER

Open Access

Evaluating the impact of reducing POFA's particle fineness on its pozzolanic reactivity and mortar strength

Yu Xuan Liew[1], Siti Asmahani Saad[2], N. Anand[3], Kong Fah Tee[4,5*] and Siew Choo Chin[1,6*]

Abstract

This paper presents the effect of size reduction of palm oil fuel ash (POFA) in the nanoscale to improve the mortar strength. In this work, three different particle sizes of POFA prepared using the LA abrasion machine were used as a cement replacement. The physical and chemical properties, mineralogy, and morphology of all POFA specimens were studied. The effect of size reduction on the pozzolanic reactivity of POFA is also studied. The mortar mix design that contained micro and nano POFA was prepared and evaluated for its compressive and flexural properties at the ages of 7, 28, 56, and 90 days. Response surface methodology was used to evaluate the relationship between the factors (cement replacement) and responses (compressive and flexural strength), aiming to find the best mix design. The grinding method in this work produced POFA as small as 110 nm. The nano POFAs were observed to have better pozzolanic reactivity compared to micro POFA. The results show that nano POFA increased the mortar strength activity index by up to 20% compared to micro POFA. The best mix design was found using a combination of 10 and 3% of micro and nano POFA as cement replacement. The best mix design shows excellent early compressive strength (7 days) compared to other mixes, although the difference in long-term compressive strength is insignificant. Similar findings were observed for the flexural strength, whereby the best mix design was obtained using a combination of 10 and 3% of micro and nano POFA. This work may provide useful insight into the effect of size reduction on the pozzolanic reactivity of POFA.

Keywords Nano, Palm oil fuel ash, Los Angeles abrasion machine, Pozzolanic reactivity test, Mortar, Response surface methodology

*Correspondence:
Kong Fah Tee
tee.fah@kfupm.edu.sa; kftee2010@gmail.com
Siew Choo Chin
scchin@umpsa.edu.my
[1] Faculty of Civil Engineering Technology, Universiti Malaysia Pahang Al-Sultan Abdullah, Gambang, Pahang 26300, Malaysia
[2] Department of Civil Engineering, Kuliyyah of Engineering, IIUM, Kuala Lumpur, Selangor 53100, Malaysia
[3] Department of Civil Engineering, Karunya University, Karunya Nagar, Coimbatore 641114, India
[4] Department of Civil and Environmental Engineering, King Fahd University of Petroleum and Minerals, Dhahran 31261, Saudi Arabia
[5] Interdisciplinary Research Center for Construction and Building Materials, KFUPM, Dhahran 31261, Saudi Arabia
[6] Center for Research in Advanced Fluid and Processes (Fluid Centre), Universiti Malaysia Pahang Al-Sultan Abdullah, Gambang, Pahang 26300, Malaysia

Introduction

The expeditious development in industrialization as well as urbanization stimulated the growth of the construction industry at the rate of 8% annually, and this will escalate the demand for construction materials at the same time (Li et al. 2023). Among those construction materials, concrete which acted as the backbone of the recent construction development has been a concern since the manufacturing of Portland cement contributed 5–8% of global carbon dioxide emission from its product life cycle leading to global warming (Asghar et al. 2023; Liu et al. 2022a). The establishment of supplementary cementitious material (SCM) as admixture or cement replacement in the concrete mixture was one of those efforts which not only reduced the cement demand but also improved the concrete engineering properties (Ibrahim and Meawad 2022; Suraneni et al. 2019). Common SCMs such as slag, metakaolin, fly ash, and agricultural waste ashes have continually been studied and implemented in the market (Tee and Mostofizadeh 2021; Mostofizadeh and Tee 2021; Samad et al. 2018, 2017). Most of these common SCMs originate from the waste products of manufacturing or energy generation; thus, it also helps recycle these industrial byproducts rather than burying them.

The SCM was rich in content of silica and alumina, and these components were later reacted with calcium hydroxide (CH) to produce the products that promoted the strength development of concrete. This process is known as the pozzolanic reaction and occurs at a slower age due to the late formation of CH that is produced from the hydration of cement. However, difficulties were increasing in using these received waste products as SCMs due to the variability in quality, especially in the case of agricultural waste ash. The quality of SCMs can be measured by their pozzolanic or cementitious reactivity level in the cement mixture, while those influencing factors were its physical as well as chemical properties, mineralogy, and morphology (Pacewska and Wilińska 2020; Panesar and Zhang 2020; Ismail et al 2020). Reasons such as the source of the agriculture that is subject to the burning process, different ash collecting points, temperature as well as the duration of the incineration process, a treatment that is conducted on the ash, and so on will affect the SCMs quality. So, several activation methods such as mechanical activation, chemical activation, thermal activation, or a combination of different activation methods have been introduced to improve SCMs' reactivity (Liu et al. 2022b; Wilińska and Pacewska 2018). These treatments could improve the particle properties of the SCM by reducing the particle fineness, increasing those particles' specific surface area, increasing the content of silica, enhancing the mineral properties, and modifying the morphology of particles. Size reduction of SCMs was studied in the past, and enhancement in mortar strength was reported (Sun et al. 2021; Zeyad et al. 2021; Mangi et al. 2019). For instance, Mangi et al. (2019) reported enhancement in compressive strength and concrete porosity as the SCM size was reduced. In detail, the SCM with finer particles had better pozzolanic reactivity due to the improvement in the heterogeneous nucleation effect and speed up the chemical reaction with calcium hydroxide ($CaOH_2$). Moreover, finer SCM has a superior particle filling effect which leads to the improvement in concrete or mortar strength especially at early curing ages (Sun et al. 2021; Zeyad et al. 2021). In most cases, the comparison is limited to just two particle sizes, and a limited study on the effect of mixed particle sizes on mortar strength was made. Thus, this work focused on evaluating the effect of various SCM sizes and the effect of mix size SCM on the mortar strength, especially the strength at early curing ages (7 days).

Thus, nanoscale SCM in the particle sizes range of 100 to 1 nm has been introduced in the cement mixture. Nano silica was one of the famous nanomaterials that were used as mineral additives in previous research. Given the extremely fine particle size and high specific surface area of the nanoscale SCM, it successfully promoted the early-age compressive strength of the pozzolan-based mortar, reducing the setting time of the cementitious mixture and accelerating the hydration process (Liu et al. 2022b). The top-down approach nanomaterial preparation method has been performed in past research on palm oil fuel ash (POFA) for improving its reactivity and thus improving the POFA-based cementitious mixture's engineering properties (Hassan et al. 2017; Rajak et al. 2019; Tang et al. 2019; Wi et al., 2018a). POFA was one of the agricultural wastes that were rich in silica content and can be used as a potential pozzolanic material; however, the inconsistency of the SiO content in the POFA was reported from different research which range from 35 to 69% (Al-Kutti et al. 2018; Alsubari et al., 2018a; Chalee et al. 2021; Hossain et al. 2020; Muthusamy et al. 2019). In past research, the high-energy ball milling machine with higher grinding speed was frequently used in grinding the micro-scale POFA until the nanoscale and reported the nano-scale POFA had particle size ranging from 20 to 150 nm (Hassan et al. 2020; Rajak et al. 2015; Samadi et al. 2020; Tang et al. 2019; Wi et al., 2018a). Only Hamada et al. (2020a, b) proposed using the Los Angeles (LA) abrasion machine which had a low grinding speed for grinding the micro-scale POFA to the nanoscale; however, the produced POFA only had a particle size of 982 nm which is far bigger than the "standard" nanomaterial. Judging on the easier accessibility of the LA abrasion machine than the high-energy

grinding machine, it is worth noting to further improve the grinding parameters to use the LA abrasion machine-producing nanoscale POFA.

Those past reported mix designs used nano POFA as cement replacement at different replacement rates that range between 20 and 80% (Hussin et al. 2015; Lim et al. 2018; Rajak et al. 2021; Samadi et al. 2020; Wi et al., 2018a). On the other side, the concrete mix design contained nano POFA in a lower dosage around 1 to 3% (Tang 2018; Wan Hassan et al., 2020a) and incorporated micro-scale POFA compared to the mortar mix design. Observing the relative compressive strength of this nano POFA-based concrete or mortar, the reported optimum replacement rate of nano POFA was around 40% with a relative strength of 123 to 135% at late curing ages (Samadi et al. 2020), while the concrete that contained the combination of 10% micro and 1 to 3% nano POFA had a relative strength of about 103 to 103.7% at late curing ages. Indeed, using high replacement of nano POFA in concrete or mortar mix design improved the strength of concrete and mortar at late curing ages, but looking at the economical aspect, this mix design was not relevant since the time- and energy-consuming of the nano POFA preparation method. Hence, using a lower dosage of nano POFA and incorporating the appropriate amount of micro-scale POFA were more sustainable. A similar mix design that used optimal dosage (ranging from 1 to 5%) of nanomaterial and cooperated with appropriate micro-scale SCMs was proposed to obtain better properties (Abdalla et al. 2022; Monteiro et al. 2022).

In short, the potential of using an LA abrasion machine with a slow grinding speed to produce nano POFA has rarely been explored. Moreover, the nano POFA that had a particle size in the range between 150 and 982 nm has rarely been discovered for their pozzolanic reactivity as well as impact as a cement replacement in blended cementitious mixtures. This paper aimed to produce the nano POFA by using the LA abrasion machine and later investigated the impact of reducing particle size on the POFA's pozzolanic reactivity as well as its role as cement replacement in mortar. To produce "nano" scale POFA, modified grinding parameters were designed that take count the impacts of the steel ball size, weight ratio of steel ball to POFA, and grinding periods. Those produced nano POFAs' properties will be evaluated in terms of physical properties, chemical properties, mineralogy, and morphology. Pozzolanic assessments such as the Frattini test, strength activity index, Chapelle test, and thermogravimetric analysis will be carried out to distinguish the impact of fineness on the pozzolanic reaction of POFA. Later, the mortar mix design that contained the combination of micro and three types of nano POFA was prepared and subjected to compressive strength and flexural strength at the curing ages of 7 to 90 days. The influence of the different types of nano POFA that resulted from various grinding cycles as well as the combination micro plus nano POFA mix design was analyzed and expressed these factors' relationship with the aid of statistical test setup and response surface methodology (RSM).

Material and methods

Material

Cement

The grade 52.5 N ordinary Portland cement (OPC) was purchased from local suppliers and used in this study. The OPC in this work is similar to that used by Chin et al. (2018) and Chin et al. (2019). The manufacturing of this cement was claimed to be fulfilling the ME EN 197–1:2014 CEM1 52.5 N standards. The manufacturer also provided the details for the initial and final setting times which were 153 min and 184 min.

Palm oil fuel ash (POFA)

The top-down approach of the nanomaterial preparation method was applied by using the LA abrasion machine. Two stages of mechanical activation and thermal activation were carried out on the received POFA to improve its reactivity. The raw POFA was provided by the local palm oil mill located at Gambang, Pahang, Malaysia, and stored at Concrete Laboratory, University Malaysia Pahang Al-Sultan Abdullah. In the very first stage, the raw POFA was dried in the oven at the temperature of 100 ± 5 °C for 1 day to remove water moisture that was trapped in it, and the passing residue was obtained after being sieved through a 300-μm sieve. Next, the sieved POFA was ground by using the Los Angeles abrasion machine until 90% of the ground ash was passing the 45-μm sieve (Aggregates, 2013). The grinding parameters for the micro POFA were maintained at the POFA's weight of 3 kg per round, and grinding cycles were 10,500 times. The wet sieving method has been used for ensuring the passing size of ground POFA, where 100-g samples were obtained from each batch of ground POFA and sieved under running water. The retained ash was dried, weighed, and calculated for the passing rates.

The ground micro-scale POFA was later subjected to thermal activation by using an electrical furnace at the temperature of 600 °C for 2 h. The color of the completed treated micro POFA should be gray color from black color as shown in Fig. 1a, b, c which indicates the unburned carbon has been removed from the POFA (Hamada et al. 2022; Wan Hassan et al., 2020). A second stage grinding process was carried out to produce the nano-scale POFA. Still using the LA abrasion machine, these grinding parameters: weight ratio of steel ball to micro POFA at 10:1 and diameters of steel ball used were

Fig. 1 The black color of ground POFA (**a**) changes to gray color micro POFA (**b**), and (**c**) is the 50k nano POFA

50 mm and 20 mm and were kept constant, but the grinding periods were designed at 50,000, 80,000, and 110,000 cycles. Each batch of the nano POFA was collected and evaluated in different properties.

Fine aggregate

The fine aggregate was obtained from a local supplier in Pahang, Malaysia, while the sand that passed through a 1.18-mm sieve and retained at 600-µm sieve was used in the mortar mix design (Standard 2008). The sand is sourced from the Kuantan River, similar to that of Teara et al. (2019). The fine modulus of the sand was 2.44.

Characteristics of POFA

The physical properties, chemical properties, morphology, and mineralogy of all types of POFA were carried out. The particle size of all nano POFAs was confirmed by using a particle size analyzer, and the field emission scanning electron microscopy (FESEM) was carried out at all nano POFAs to provide the morphology detail as well as provided supporting information for the particle size. In addition, the specific gravity of all POFA was carried out by referring to ASTM C188. Chemical properties of untreated POFA, micro POFA, and nano POFA were evaluated by using X-ray fluorescence (XRF) to identify the effect of mechanical activation and thermal activation. Loss on ignition value of all types of POFA was determined by referring to the method in ASTM (2005).

Pozzolanic reactivity assessments of POFAs

Various types of pozzolanic assessment have been used for evaluating the pozzolanic reaction of SCM whether it was direct or indirect methods. In this paper, the following pozzolanic reactivity tests, viz., Frattini test, strength activity index (SAI), modified Chapelle test, and thermogravimetric analysis (TGA), were carried out on the micro POFA, 50k nano POFA, 80k nano POFA, and 110k nano POFA. Frattini test was performed on micro POFA, and all nano POFAs by following the standards BS EN 196–5 (EN, 2005) and the replacement rates of 20% were used to replace cement with various types of POFA. For the SAI test, the mortar samples were prepared following the ASTM C311, and the replacement rate of 20% was used as recommended in the standards for the micro POFA and all nano POFAs. The compressive test was conducted on those samples at the curing age of 7 and 28 days, and results were later calculated in SAI value. In the modified Chapelle test, the 250-ml solution that contained 1 g of the POFA sample and 2 g of calcium oxide CaO was heated at 90 °C for 16 h with continuous stirring (Ferraz et al. 2015). The non-consumed calcium hydroxide (CH) was quantified later against the dilute hydrochloride acid solution, and the result was expressed in milligram of fixed CH by a gram of sample. TGA was conducted on the cement paste to examine the amount of formed cementitious material at the respective phase (Martins et al. 2021). While the calcium hydroxide (CH) content in the cement paste contained the optimum combination of micro and nano POFA, but the difference in the type of nano POFA was focused on in this paper. The water-cured cement paste with curing ages of 7 and 90 days was subjected to the solvent-exchange process by using isopropanol and drying process later. Crushed cement pastes with particle sizes less than 45 µm were undergone a TGA test by using the instrument, PerkinElmer TGA 4000. The sample was heated from temperature of 35 °C to 850 °C, with a heating rate of 10 °C/min, and using nitrogen with a flow rate of 5 mL/min. Based on past studies, the content of CH was quantified based on the weight loss of the sample between the temperature range of 400 to 500 °C by using Eq. 1 (Snehal and Das 2022).

$$\text{CH } \% = (\%W_{\text{CH}}) \times M_1/M_2 \quad (1)$$

CH % is the mass content of CH in percentage

W_{CH} is the weight loss percentage of CH from the TGA curve and weight loss derivative curve

M_1 is the molecular mass of CH with the value of 74 g/mol

M_2 is the molecular mass of water with the value of 18 g/mol

Incorporating the nano POFA and micro POFA in mortar

The replacement rates of the micro and nano POFA combination were introduced in the mortar mix design as shown in Table 1, while the mortar mix was designed, material preparation, mixing, and testing based on ASTM C109-2021 standards. The following mix design criteria were designed as mentioned in standards, viz., sand to cement ratio was 2.75:1, and water to cement ratio was 0.485. The mortar cube that was later subjected to the compressive test had a size of 50 mm × 50 mm × 50 mm (L × W × H), while the mortar prisms had the size of 160 mm × 40 mm × 40 mm (L × W × H) and were prepared for the flexural strength test by referring to the standard, ASTM C348. All mortar cubes or prisms were water cured for the curing ages of 7, 28, 56, and 90 days. The flowability of the freshly mixed mortar was evaluated based on the ASTM C109-2021 standards. The freshly mixed control mortar was maintained at the flow table value of 110 ± 5. Hardened properties of mortar were examined in terms of compressive strength and flexural strength at the respective curing ages.

To evaluate the interaction between the factors and responses, the response surface methodology (RSM) version 12.0.12, a mathematical and statistics method was applied. The Design-Expert software was used to perform the RSM statistical test setup, while this software provided the equations to express the relationship between the variables and provided the most desired solution (Wan Hassan et al., 2020b). The factor variables included the replacement rate of micro POFA, nano POFA, and the grinding cycles, while the hardened properties at all curing ages were covered in the response variables. These equations were subjected to analysis of variance (ANOVA) and expressed in terms of prediction models, model terms, modal significance, coefficient of determination (R^2), and probability (p-value) at a 95% confidence level.

Result and discussion

Properties of POFA

Using the LA abrasion with modified grinding parameters significantly changed the physical properties of POFA as presented in Table 2. A remarkable change occurred in the particle size of all types of POFA from micro to nanoscale. The proposed grinding parameter was able to reduce the POFA particle until ranging from 529 to 103 nm by increasing the grinding cycles from 50 to 110k. The nano POFA with the size of 103 nm was produced, and this is close to the requirement of a nanomaterial (Armarego 2022). The specific gravity of the micro POFA and all types of nano POFA ranged between 2.19 and 2.54 which was close to the value reported by Samadi et al. (2020). These values were lower than the OPC's value which showed these POFA were lighter than the OPC. After conducting the thermal and mechanical activation on the raw POFA, the LOI values of micro

Table 1 Mortar mix design

Mix no	Micro POFA replacement rate (kg per batch sample)	50k, 80k, or 110k cycles nano POFA replacement rate dosage (kg per batch sample)	Cement amount (kg per batch sample)	Water (kg per batch sample)	Sand (kg per batch sample)
M0	0	0	3	1.455	8.25
M10N1	0.3	0.03			
M10N2	0.3	0.06			
M10N3	0.3	0.09			
M20N1	0.6	0.03			
M20N2	0.6	0.06			
M20N3	0.6	0.09			
M30N1	0.9	0.03			
M30N2	0.9	0.06			
M30N3	0.9	0.09			

Table 2 Physical properties of various types of POFA

Properties	Micro POFA	50k nPOFA	80k nPOFA	110k nPOFA
Specific gravity	2.19	2.56	2.53	2.54
Average particle size	90% passing 45-μm sieve	529 nm	325 nm	103.1 nm

Table 3 Chemical composition of raw, micro, and all types of nano POFA

Properties	Raw POFA (%)	Micro POFA (%)	50k nano POFA (%)	80k nano POFA (%)	110k nano POFA (%)
SiO_2	32.1	58	59.4	58.6	58.8
Al_2O_3	2.28	6.36	6.08	7.08	6.05
Fe_2O_3	3.5	6.6	8.51	9.7	9.66
CaO	7.28	9.03	8.24	8.04	8.21
MgO	2.99	2.96	3.67	2.68	3.57
Na_2O	0.097	0.206	0.251	0.226	0.27
K_2O	7.27	9.49	8.37	8.01	8.13
SO_3	1.14	1.58	1.00	1.02	0.93
Sum of SiO_2, Al_2O_3, Fe_2O_3	37.88	70.96	73.99	75.38	74.51

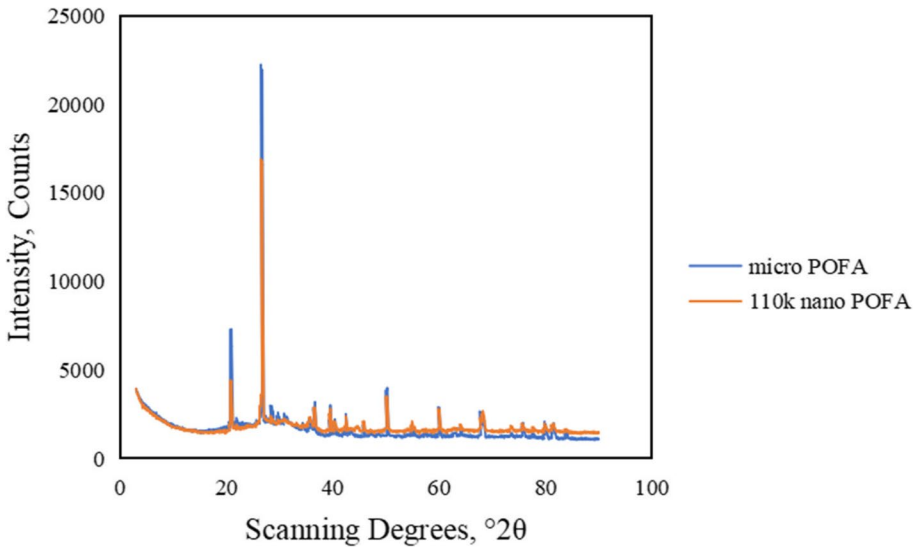

Fig. 2 XRD results in comparison for the micro and 110k nano POFA

POFA and all types of nano POFA were in the range of 3 to 4.85%, which were still lower than the requirement LOI value, 6% in ASTM C618.

Table 3 presents the chemical composition of the raw, micro, and nano POFA. After conducting the thermal activation, the silica content of micro POFA was improved by up to 58%, and also, the sum of the chemical content of Al_2O_3, SiO_2, and Fe_2O_3 increased to 70.96 reaching the bottom line of pozzolan material in ASTM C618. Further, grinding the micro POFA until nano POFA still improves the sum of chemical composition until reaching the range between 73.99 and 75.38%. Both micro and all types of nano POFA could be classified as class F and C pozzolan which aligned with previous studies (Oyehan et al. 2022; Samadi et al. 2020).

The comparison of the XRD results of the micro and 110k nano POFA is presented in Fig. 2. Table 4 presents the summary of the peak intensity of each type of POFA from XRD analysis. Generally, both types of POFA had a similar XRD intensity trend and the degree to which the peaks were located. The major crystalline phase of micro and all nano POFAs was quartz (SiO_2),

Table 4 Summary of the XRD's peak intensity of each type of POFA

Types of POFA	First peak intensity at 21° (counts)	Highest peak intensity at 26 to 27° (counts)
Micro POFA	4447.78	21,936.56
50k nano POFA	1410.33	7596.68
80k nano POFA	1281.47	7042.49
110k nano POFA	2047.87	11,237.63

while the presence of the diffractive halos pattern at the angle between 19 and 36° indicated the low crystallinity (glassy phase) of them. This result was aligned with the past studies, while conducting the mechanical grinding and thermal activation of POFA at the temperature of 600 °C for 2 h did not affect the mineral phase of POFA (Samadi et al. 2020; Zeyad et al. 2017). Apart from that, a significantly lower XRD peak intensity was observed in all nano POFAs than in the micro POFA. A similar result was reported in (Kim et al. (2019) due to the decrease in the POFA's crystallinity after being ground until a finer scale. Cheng et al. (Cheng et al. (2021) further explained the combination of suitable thermal activation, and mechanical grinding could reduce the peak in XRD and convert the composition into an amorphous phase. In addition, the peak shape of the 110k nano POFA was found to be broader as compared to the micro POFA's XRD peak shape which also suggests the lower crystallite size as well as possible higher amorphous in 110k nano POFA (Cho et al. 2019). Thus, the suspected improvement of amorphous in the nano POFAs due to the grinding process will be justified in the pozzolanic assessments.

The morphology of the 50k, 80k, and 110k nano POFA is presented in Figs. 3, 4, and 5. The particle of 50k nano POFA was observed in an angular and irregular shape, while bigger particles were found, and smaller particles were attached around them. For the 80k nano POFA, lesser amounts of bigger size particles were noticed than the 50k nano POFA, and lesser agglomeration occurred in those particles. Agglomeration condition has still been detected in the 110k nano POFA; however, these particles were found in an angular and closer to a circular shape.

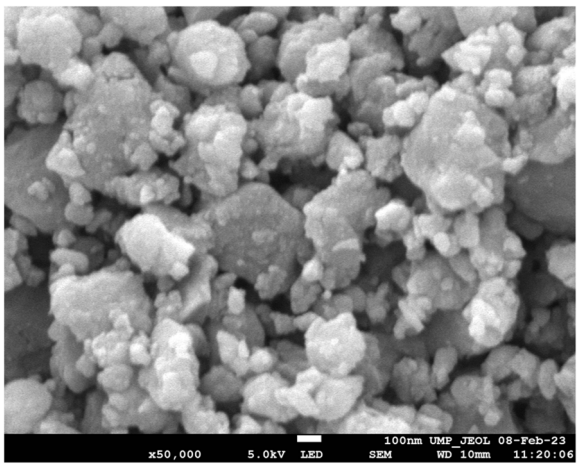

Fig. 4 Morphology of 80k nano POFA particles in 50,000 magnifications

Pozzolanic assessments of various POFA

Frattini test

Figure 6 presents the result of various types of POFA's pozzolanic reactivity through the standards BE EN 196–5. The aqueous solution from the cement pastes was subjected to titration for CH and OH concentration, and the determination of the material as pozzolanic depended on the CH solubility curve. At the curing age of 15 days, all POFAs' results were located below the CH solubility curve which indicated these POFA had pozzolanic reactivity. In the reference sample, cement paste without POFA replacement showed inactive since it was located above the line. Unfortunately, this test has only been limited in identifying the absence of pozzolanic reactivity in the studied material, while investigating the influences of pozzolanic reactivity due to the properties of pozzolan

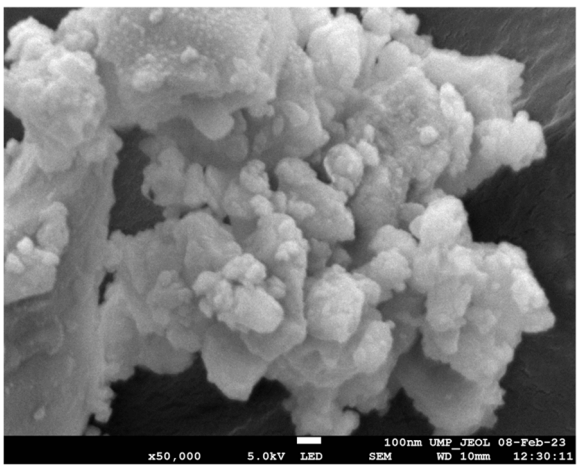

Fig. 3 Morphology of 50k nano POFA particles in 50,000 magnifications

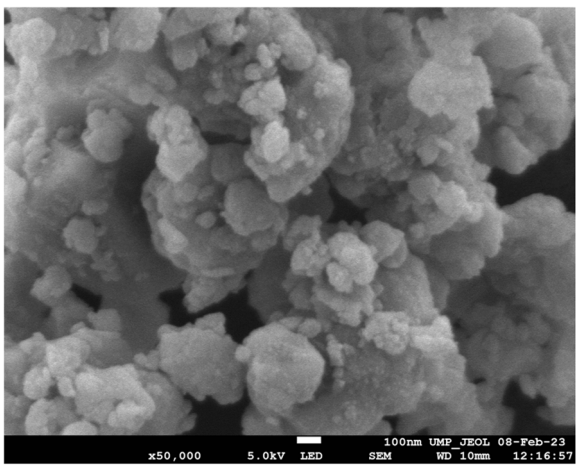

Fig. 5 Morphology of 110k nano POFA in 50,000 magnifications

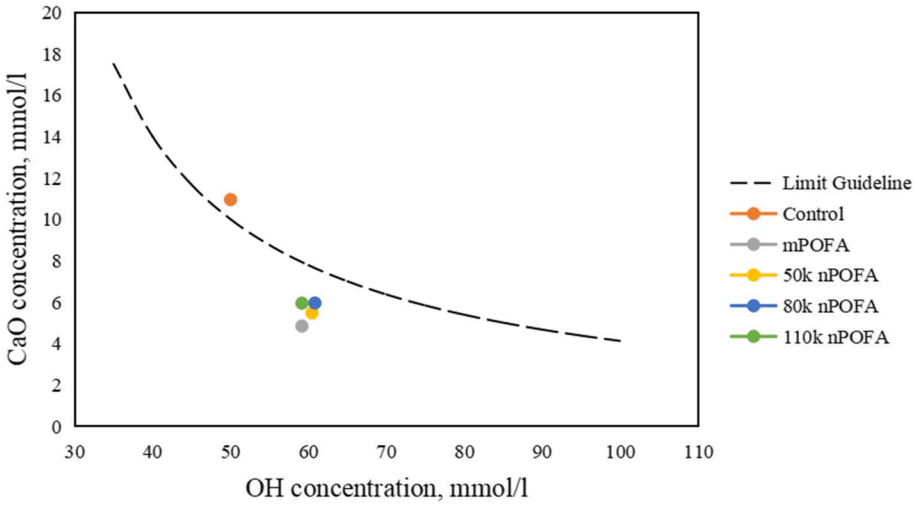

Fig. 6 Frattini test for indicating the pozzolanic reactivity of POFA

material was less concerned in this test (Kamalakar Mali and Nanthagopalan 2021Nanthagopalan 2021).

Strength activity index (SAI)

The SAIs of the mortar that contained either micro POFA, 50k, 80k, or 110k nano POFA were displayed in Fig. 7. All POFA-based mortar's SAI values in both curing ages surpassed the minimum value of 75%, stated in ASTM C618 for considering the POFA as pozzolanic material (K. and Das, 2022). Although the micro POFA mortar had an SAI value greater than the minimum requirement, its value was the lowest among all samples in the 7 and 28 days. Due to having a larger particle size and coarser particles as observed in micro POFA than the nano POFA, the SAI values of 84.5% and 87.3% were found at the 7 and 28 days. Moreover, the dilution

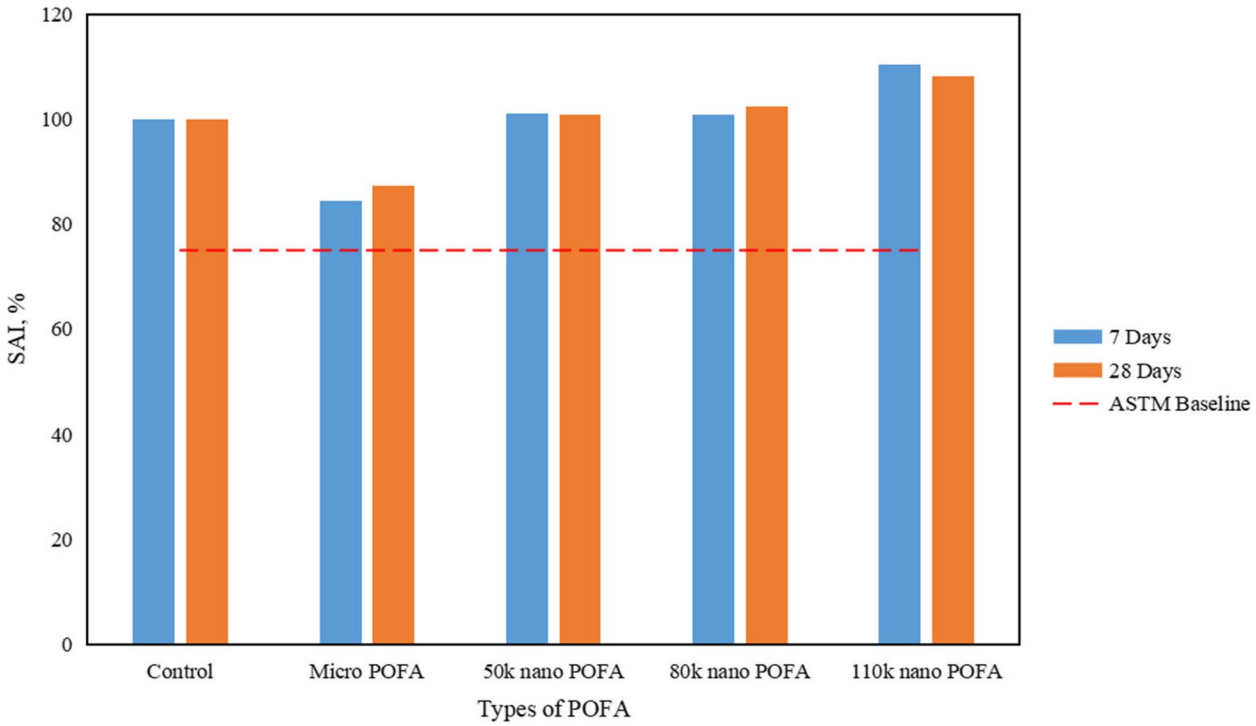

Fig. 7 Strength activity index for mortar containing micro and all types of nano POFA

effect due to the cement replacement by micro POFA as well as the delayed onset of the pozzolanic reaction of micro POFA led to lower SAI (Lim et al. 2015). In contrast, incorporating the nano POFA in mortar mix design was found to increase the SAI value at both curing ages, while finer particle size of nano POFA improved the 7-day SAI the most. As evidence, the 110k nano POFA which had the finest particle size led to the highest SAI that ranged from 110 to 108.13% at both curing ages. The smaller particle size of the 80k nano POFA than the 50k nano POFA led to a better 28-day SAI value in the 80k nano POFA-based sample. This proved that reducing the SCM's particle fineness could improve the SAI value, and similar trends have also been reported in Jaturapitakkul et al. (2011), Lim et al. (2015), Rajak et al. (2019), Samadi et al. (2020), and Sinsiri et al. (2012). A nanoscale particle of the pozzolanic material could provide a greater filler effect and also act as the potential nucleation site in a mortar mixture. In consequence, the rate of pozzolanic reaction has been accelerated and promoted the development of secondary calcium silicate hydrate (CSH) that contributed to the mortar-hardened properties (Rajak et al. 2019). This is reflected in the improvement of all nano POFA-based mortars' SAI greater than control at both curing ages. In this assessment, the impact of particle size was found to be more influencing where finer particles in the POFA led to better SAI value which also aligned with the finding in Kamalakar and Prakash (2021) and Pormmoon et al. (2021).

Modified Chapelle test

The modified Chapelle test could quantify the fixed calcium hydroxide (CH) consumption amount in the material and determine its pozzolanic reactivity. The minimum consumption value for classifying the material as pozzolan was 436 mg CH/g in Borges et al. (2021). However, a higher range of CH consumption value that ranged from 700 mg/g and above was found to provide better pozzolanic reactivity due to the low crystallinity phases, higher SSA, and soluble fraction of the SCM (Andreão et al. 2020; Cordeiro et al. 2019; Mali and Nanthagopalan 2021). Figure 8 presents the Chapelle test's result for all types of POFA. It shows that all types of POFA could be classified as pozzolan since all POFAs' CH consumption values ranged from 483 to 796 mg/g exceeding the minimum requirement. On the other hand, all those nanoscales POFA could be considered to have better pozzolanic reaction since those nano POFA had values ranging from 766 to 796 mg/g which closed or surpassed the values from those reported high pozzolanic reactivity SCM. The lower peak intensity of the nano POFA from the XRD result also could confirm the improvement of amorphous content due to the grinding process and led to the higher consumption of CH than micro POFA. In this assessment, the 80k nano POFA had consumed the most amount of CH than the 50k and 110k nano POFA, but the variance was not significantly different showing a similar level of pozzolanic reactivity among these nanoscale POFA. This may be attributed to the similarity of these nano POFA's particle characteristics such as the low crystallinity phase, similar chemical content, and close range of the specific surface area (Kamalakar and Prakash 2021; Martins et al. 2021).

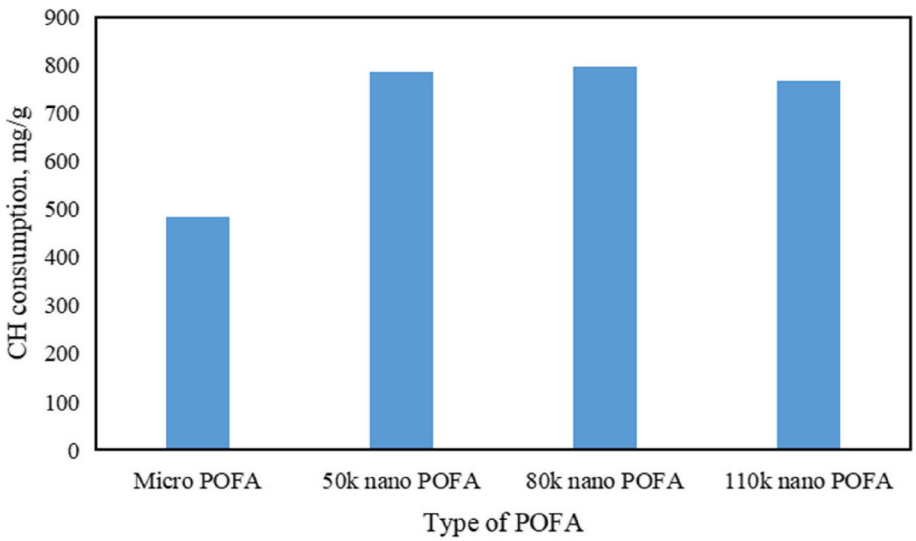

Fig. 8 Modified Chapelle test result of various types of POFA

Thermogravimetric analysis

The cement paste that contained the optimum ternary mix design but differed in the type of nano POFA was subjected to thermogravimetric analysis (TGA) at the curing age of 7 and 90 days. Thus, the difference between the three types of nano POFA in terms of pozzolanic reactivity was evaluated by observing the reduction of CH from the TGA results. All the TGA and derivatives weight curves of cement pastes with all types of nano POFA on the curing ages of 7 and 90 days are presented in Fig. 9a to d. From Fig. 9b and d, it can be observed three endothermic peaks that are located at different temperature ranges. The first endothermic peak located at the temperature ranges of 40 to 200 °C represented the weight loss of water and decomposition of CSH, ettringite, and gypsum, while the second peak observed at the temperature range of 400 to 500 °C is the dihydroxylation of CH, and the last peak that represents the weight loss of calcium carbonate is located at the range of 550 to 800 °C (Men et al. 2022; Wang et al. 2021). The mass content of CH of each cement paste at the curing ages of 7 and 90 days is calculated by using Eq. 1 and summarized in Table 5.

The control sample with no replacement of POFA had the highest CH content at both curing ages. On the other hand, the POFA-based cement paste had a lesser amount of CH due to the replacement of cement in those POFA-based cement pastes and led to a lesser amount of CH produced from the hydration process in cement (Altwair et al. 2011). In addition, the amount of CH in the control cement paste was observed to increase from day 7 to day 90 due to the continuous hydration process. On the other hand, the CH content of nano POFAs was found to reduce or remain at the day of 90 which showed the consumption of CH by nano POFA (Wi et al., 2018a). The 80k nano POFA cement paste had the lowest CH content at all times, later followed by the 50k nano POFA and the 110k nano POFA which had a higher CH content. The lower CH content in the 80k nano POFA cement paste indicated the better pozzolanic reactivity of it, and more CH was consumed than other nano POFAs. The TGA result was found to have a close correlation to the nano POFA's XRD peak intensity as compared to other particle characteristics such as particle size and chemical properties. The XRD result reflected the mineral phase of nano POFA to have a smaller crystallinity size and possibly higher amorphousness than the micro POFA (Cheng et al. 2021; Kim et al. 2019). The 80k nano POFA had the lowest XRD peak intensity which indicated the low crystallinity phase and possibly more amorphousness in its mineral phase than the 50k and 110k nano POFA (Walker and Pavia, 2011). The higher amorphous structure of SCM tended to be more reactive than those with more crystalline due to the superior mobility and superficial location of their atoms (Skibsted and Snellings 2019; Walker and Pavia, 2011). Thus, the 80k nano POFA had greater reactivity and consumed more CH as compared to the other types of nano POFA in this work.

Evaluating the pozzolanic reactivity of various types of POFA in different pozzolanic reactivity assessments

The different types of POFA were found to have different pozzolanic reactivity due to their physiochemical and mineralogical properties (Snehal and Das, 2022). In this paper, four different pozzolanic tests were carried out to evaluate the reactivity of POFA with different particle properties in terms of compressive strength, quantity of CH in aqueous solution in contact with hydrated cement paste, amount of CH that has been consumed by pozzolan from a controlled amount, and the amount of CH in the hydrated cement paste that contained ternary mix design. Due to the different principles among those proposed assessments, the reactivity of all types of POFA differed in each test. Micro and all types of nano POFA were shown to have pozzolanic reactivity through the Frattini test. From the SAI and Chapelle test, all types of nano POFA had better reactivity than the micro POFA due to their smaller particle size and lower crystallinity of quartz. For comparing the reactivity among those three types of nano POFA, the correlation between SAI, Chapelle test, and TGA test was analyzed as shown in Fig. 10.

A closer correlation was found between the TGA and Chapelle test with the R^2 value of 0.8681. This indicates that the 80k nano POFA was more reactive than other nano POFAs in the TGA and Chapelle test due to its mineralogical properties. On the other hand, the correlation between the Chapelle test and the SAI test was lower, and the 110k nano POFA was found to perform better in the SAI test. Hence, it can be predicted that the particle size of nano POFA had a larger influence on compressive strength which differs from the TGA and Chapelle test.

Impact of using micro and various types of nano POFA in mortar

Compressive strength of POFA-based mortar

The compressive strength of mortar containing micro and different types of nano POFA is presented in Fig. 11a to d for the curing ages of 7, 28, 56, and 90 days, respectively. It has been observed that the changes in the replacement rate of micro POFA impacted the mortar's compressive strength significantly, especially in the early curing ages. Several researchers also reported a comparable strength reduction at the range of 4.6 to 57% in the POFA-based concrete or mortar that contained micro POFA replacement rates at 10 to 30% (Alnahhal et al.

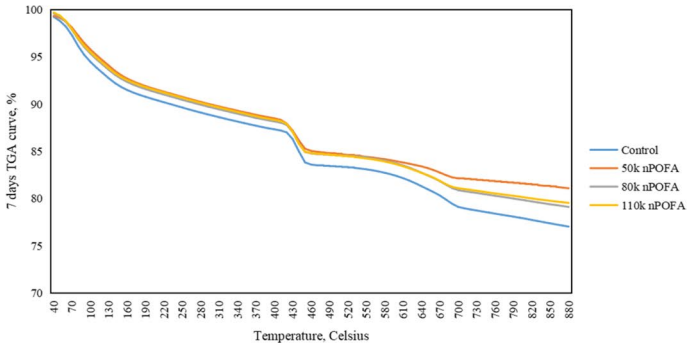

(a) Summary of the TGA curve of cement paste that either controls or contains three types of nano POFA at the 7-day curing age.

(b) Summary of the derivative weight curve of cement paste that either controls or contains three types of nano POFA at the 7-day curing age.

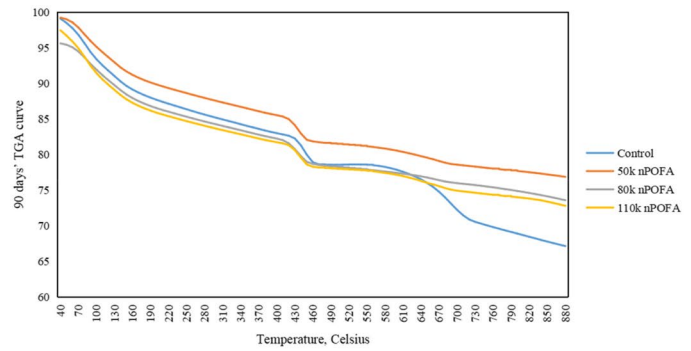

(c) Summary of the TGA curve of cement paste that either controls or contains three types of nano POFA at the 90-day curing age.

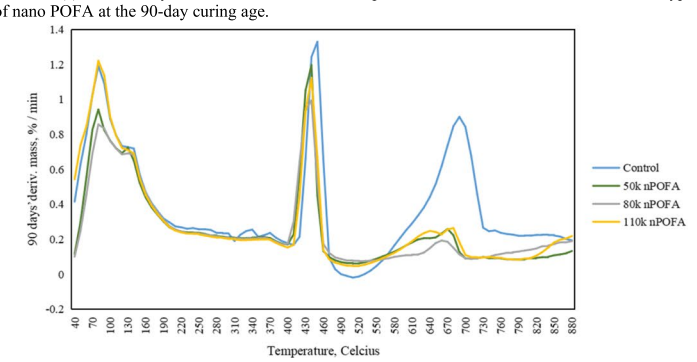

(d) Summary of the derivative weight curve of cement paste that either controls or contains three types of nano POFA at the 90-day curing age.

Fig. 9 **a** Summary of the TGA curve of cement paste that either controls or contains three types of nano POFA at the 7-day curing age. **b** Summary of the derivative weight curve of cement paste that either controls or contains three types of nano POFA at the 7-day curing age. **c** Summary of the TGA curve of cement paste that either controls or contains three types of nano POFA at the 90-day curing age. **d** Summary of the derivative weight curve of cement paste that either controls or contains three types of nano POFA at the 90-day curing age

Table 5 Summary of the CH content of each cement paste at the age of 7 and 90 days

Types of POFA	Mass loss of CH between 400 and 500 °C at 7 days (%)	7-day CH content (%)	Mass loss of CH between 400 and 500 °C at 90 days (%)	90-day CH content (%)	Changes of CH content
Control	3.41	14.02	3.65	15.00	Increased
50k nano POFA	2.90	11.92	2.90	11.92	Unchanged
80k nano POFA	2.86	11.75	2.61	10.73	Decreased
110k nano POFA	3.1	12.74	3.03	12.45	Decreased

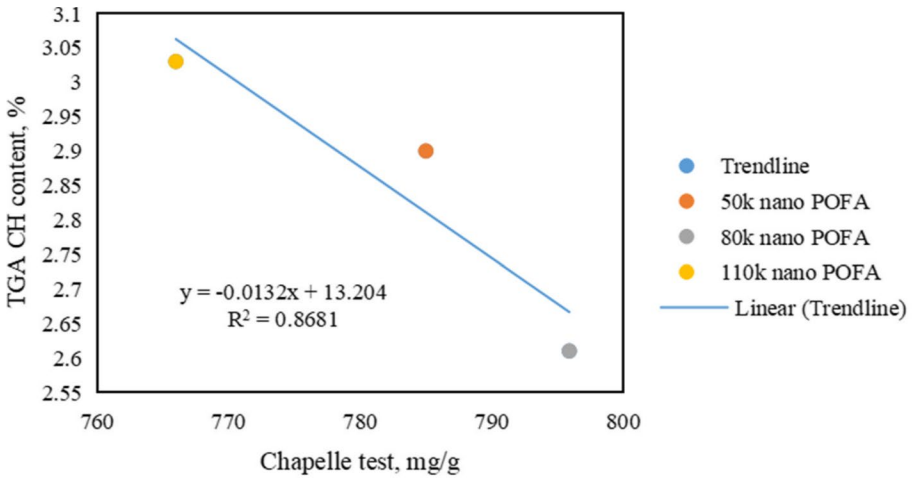

(a) Correlation plot between TGA and Chapelle test.

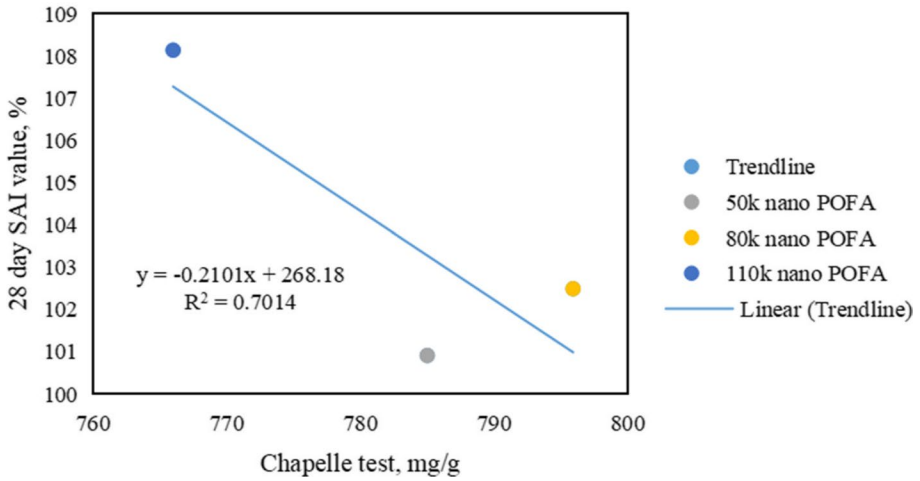

(b) Correlation plot between SAI on 28 days and Chapelle test.

Fig. 10 **a** Correlation plot between TGA and Chapelle test. **b** Correlation plot between SAI on 28 days and Chapelle test

2021; Mohammad Hosseini et al. 2021; Norhasri et al. 2021; Rajesh et al. 2020). At 7 days, the 10% micro POFA mortar had the highest relative strength at the range of 96 to 107.5% to the control mortar, while the ranges of 83 to 89% and 76 to 79% were found in the 20% and 30% micro POFA mortar, respectively. However, the variance of the range due to the difference in micro POFA replacement rate becomes smaller at later curing ages. The 10% micro POFA mortar still maintained the relative strength at the range of 95 to 104%, but the mortar with 20% micro POFA had a relative strength ranging from 90 to 98% as well as a range of 90 to 95% in the 30% micro POFA. The

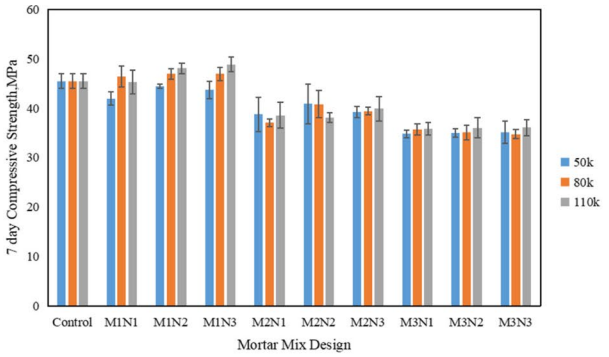

(a) Summary of the mortar's 7-day compressive strength.

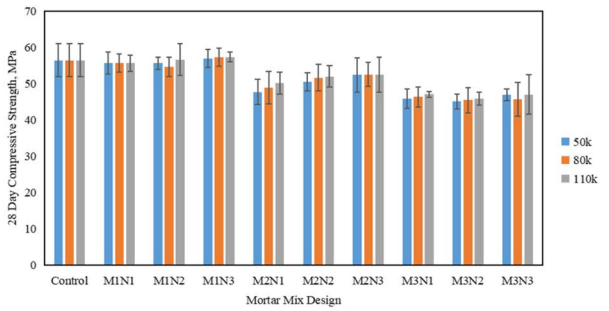

(b) Summary of the mortar's 28-day compressive strength.

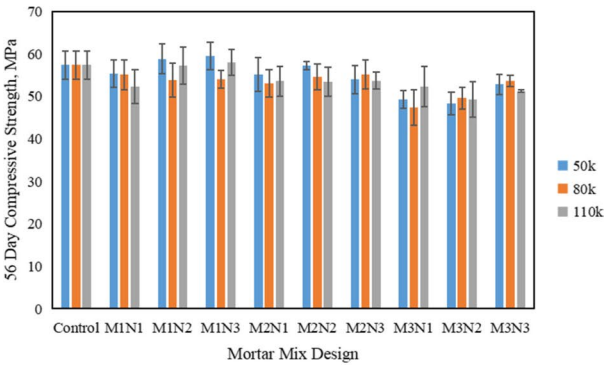

(c) Summary of the mortar's 56-day compressive strength.

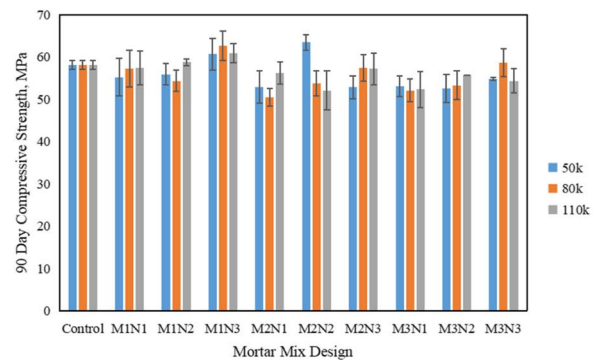

(d) Summary of the mortar's 90-day compressive strength.

Fig. 11 **a** Summary of the mortar's 7-day compressive strength. **b** Summary of the mortar's 28-day compressive strength. **c** Summary of the mortar's 56-day compressive strength. **d** Summary of the mortar's 90-day compressive strength

nature of the micro POFA has a porous structure that is suspected to absorb more free water in mortar mix and affect the hydration process (Amran et al. 2021; Raheem and Ikotun 2020). Moreover, the dilution effect due to the increasing pozzolan dosage for replacing cement was suspected to lead to the deterioration of mortar's compressive strength as the replacement of POFA increased (Hassan et al. 2020; Lim et al. 2015; Zhang et al. 2023). The lesser formation of hydrated products that contributed to the mortar strength and also the lesser concentration of CH for pozzolanic reaction were the consequences. In addition, the lower pozzolanic reactivity of the micro POFA, which has been confirmed in earlier assessments, also led to lower compressive strength at early curing ages. The findings in Alabduljabbar et al. (2021) also suggest the lower strength of POFA-based concrete due to the slower pozzolanic reaction. When pozzolanic reaction from micro POFA took place at later curing ages, the mortar's compressive strength increased and became closer to the control which can be observed in mortar with 20 or 30% micro POFA.

In contrast, increasing the dosage of nano POFA up to 2–3% in the mortar mixture was found to improve the mortar's strength despite considering its grinding cycles and replacement rate of micro POFA. As evidence, the mortar that contained the replacement rate of 10% micro and 3% nano POFA had relative compressive strength ranging from 103 to 107.5%, 101 to 103.9%, and 104 to 107.85% greater than the control mortar at the curing age of 7, 28, and 90 days. A similar improvement in concrete's strength that contained an optimum combination of micro and nano POFA up to 3.7% was reported by Wan Hassan et al. (2020a). The inversely proportional trend between the substitution rate of micro POFA and the mortar's compressive strength especially in the early curing age was also reported in Hamada et al. (2020a, b), Lim et al. (2015), Samadi et al. (2020). The presence of micro POFA which had a more porous particle absorbed more water and thus reduced the free water for the cement hydration; as the dosage of micro POFA increased, more water was absorbed and led to a higher reduction in cement mixture (Hassan et al. 2020). In addition, increasing the replacement rate of SCM reduced the portion of cement at the same time. This led to the dilution of cement where a lesser amount of calcium hydroxide (CH) was produced from the hydration process, while the CH was needed for the pozzolanic reaction. Hence,

in a lower quantity of the pozzolanic product, CSH gel was produced and caused a reduction of the pozzolan-cement mixture's compressive strength with the replacement rate that exceeded the optimum rate (Lim et al. 2015; Samadi et al. 2020; Zhang et al. 2023). Unlike the micro POFA, a positive increment trend was found in the compressive strength of mortar as the dosage of nano POFA increased. The finer particles of nano had a superior pore-filling effect and provided an extra nucleation site for the reaction which turned up in promoting pozzolanic reactivity in the cement mixtures, especially during the early curing age (Hamada et al. 2020a, b; Rajak et al. 2019; Sobolev et al. 2023; Samadi et al., Zeyad et al. 2018). Nano POFA filled the void in mortar and reacted with CH to produce additional CSH gel which thickened the mortar matrix (Hassan et al. 2020). This explained the contribution of nano POFA to mortar strength development, especially at early curing age. Moreover, the higher pozzolanic reactivity of various nano POFA has been discovered and discussed in the "Pozzolanic assessments of various POFA" section which supported the improvement of mortar's strength that contained nano POFA.

The mortar with 110k nano POFA was consistently found to have a higher compressive strength, especially at the early curing age, followed by 80k nano POFA at the late curing age. Meanwhile, the 50k nano POFA often had a slightly lower compressive strength. This may be attributed to the particle properties of the 80k and 110k nano POFA which had finer particle size ranges as well as been observed more dispersed and lesser agglomeration in morphology test. It led to the improvement in particle packing formation in mortar mixture and contributed to better strength development (Norhasri et al. 2017; Tabish et al. 2023).

It can be concluded that the optimum combination of mortar mix design to the combination of 10% micro and 3% nano POFA had the highest compressive strength at all times. The replacement rate of micro POFA has a major impact on the mortar strength, while nano POFA helps to improve the mortar strength, especially at the replacement rate of 3%. The reduced particle size of nano POFA had the least impact due to its low replacement rate and small variance among those three types of nano POFA. However, the 110k nano POFA improved the mortar's strength the most in the early curing age, while the 80k nano POFA with a better pozzolanic reactivity promoted the mortar's strength better at late curing ages.

The flexural strength of mortar contained micro and nano POFA

Figure 12a, b, c, and d shows the flexural strength results at 7, 28, 56, and 90 days of the various mix design combinations of micro and different types of nano POFA in mortar. The mortar mix that contained the combination of 10% micro and 3% nano POFA had better flexural strength than other combinations in all curing ages. A similar tensile strength development due to the changes in micro and nano POFA replacement rate was discovered in the compressive strength development and also the trend reported in (Nur et al. 2019). This may be attributed to the unique particle characteristic of nano POFA which possessed a better pore-filling effect as well as greater pozzolanic reactivity which promoted the hardened properties of mortar, especially at an earlier age. Thus, increasing the dosage of nano POFA led to the improvement of mortar strength at all curing ages. On the other hand, increasing the micro POFA replacement rate led to a reduction in mortar strength which was attributed to its coarser particle size, higher replacement rate, and slower pozzolanic reactivity. Last but not least, the variance of mortar's flexural strength due to types of nano POFA from varied grinding cycles was also small and even lesser than that in compressive strength.

Using respond surface methodology (RSM) for analyzing and optimization

It is possible to explain the interaction between variables and responses through the response surface models with the aid of RSM and analysis of variance to predict the response (Nur et al. 2019; Waqar et al. 2023; Fang and Tee 2017). The variables included the replacement rate of micro, nano POFA, and the grinding cycles of nano POFA, while the mortar's compression strength and flexural strength at each curing age (7, 28, 56, and 90 days) were designed as responses in the modeling. Equations were formed and expressed in terms of coded factors, while the prediction response was the result of the respective equation which considered all codes' influence. Variables such as the replacement rate of micro POFA, nano POFA, and grinding cycles were denoted as Codes A, B, and C. These factors were labelled with a coefficient that ranged from positive to negative number, and the value indicated the factor's impact level in an equation. All response models were analyzed through ANOVA and presented in Tables 6, 7, 8, 9, 10, 11, 12, and 13.

The process order of those response models was selected according to software suggestion, and these analysis elements such as sum of square, degree of freedom, mean, *F*-value, and *p*-value at 95% significant level were presented to examine the factors. The significance level of the model and each factor were determined based on the *F*-value and *p*-value. Any model or factor can be considered significant only if it has a greater *F*-value as well as a lesser *p*-value (preference less than 0.05). All chosen models had a high *F*-value and a low *p*-value (lesser than 0.0001) showing the high significance of the responses.

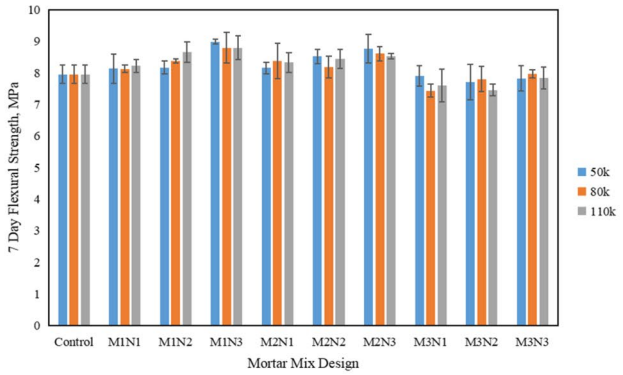

(a) Summary of the mortar's 7 days flexural strength.

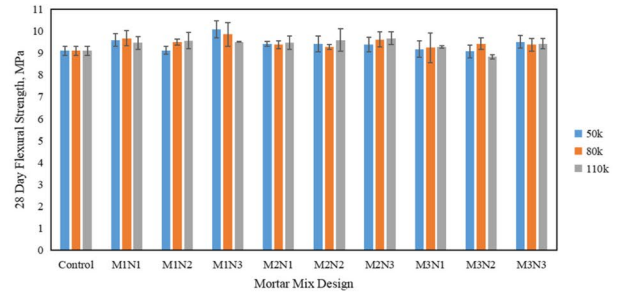

(b) Summary of the mortar's 28 days flexural strength.

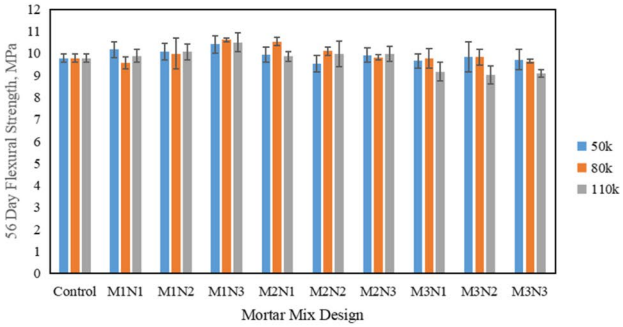

(c) Summary of the mortar's 56 days flexural strength.

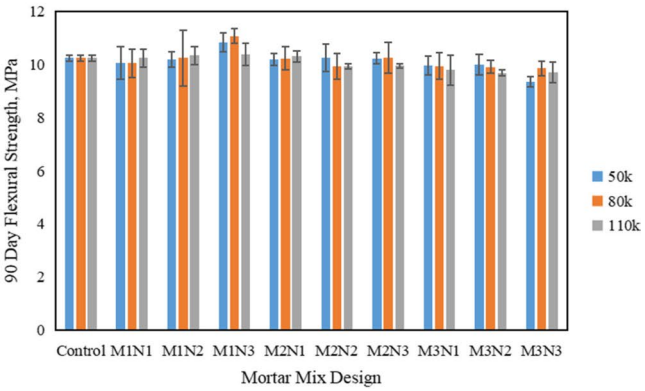

(d) Summary of the mortar's 90 days flexural strength.

Fig. 12 **a** Summary of the mortar's 7-day flexural strength. **b** Summary of the mortar's 28-day flexural strength. **c** Summary of the mortar's 56-day flexural strength. **d** Summary of the mortar's 90-day flexural strength

Table 6 The 7-day compressive strength quadratic model with ANOVA analysis

Source	Sum of square	DF	Mean square	*F*-value	*p*-value
Model	537.77	9	59.75	41.45	0.0001
A	496.69	1	496.69	344.57	0.0001
B	4.22	1	4.22	2.93	0.1053
C	9.38	1	9.38	6.51	0.0207
AB	4.11	1	4.11	2.85	0.1096
AC	6.77	1	6.77	4.69	0.0448
BC	0.93	1	0.93	0.65	0.4319
A2	12.26	1	12.26	8.51	0.0096
B2	2.77	1	2.77	1.92	0.1837
C2	0.64	1	0.64	0.44	0.5142
Residual	24.51	17	1.44		
Cor. total	562.28	26			

Table 7 The 28-day compressive strength linear model with ANOVA analysis

Source	Sum of square	DF	Mean square	*F*-value	*p*-value
Model	481.47	3	160.49	96.08	0.0001
A	454.02	1	454.02	271.82	0.0001
B	26.22	1	26.22	15.70	0.0006
C	1.23	1	1.23	0.73	0.4005
Residual	38.42	23	1.67		
Cor. total	519.88	26			

Table 8 The 56-day compressive strength linear model with ANOVA analysis

Source	Sum of square	DF	Mean square	*F*-value	*p*-value
Model	166.70	2	83.55	26.63	0.0001
A	148.89	1	148.89	47.57	0.0001
B	24.61	1	24.61	7.86	0.0103
Residual	68.86	22	3.13		
Cor. total	235.55	24			

It can be noticed that factor C, referred to as grinding cycles of nano POFA, had a lesser impact in most models compared to factors A and B which aligned with the discussion in the "Compressive strength of POFA-based mortar" and "The flexural strength of mortar contained micro and nano POFA" sections. Grinding the micro POFA with longer cycles produced the nano POFA with particle size around 100 nm which was finer than those in lesser grinding times. Indeed, the 110k nano POFA mortar had better strength especially in early curing age but in a small increment. Due to the small dosage of nano

Table 9 The 90-day compressive strength quadratic model with ANOVA analysis

Source	Sum of square	DF	Mean square	*F*-value	*p*-value
Model	184.83	5	36.97	14.28	0.0001
A	65.21	1	65.24	25.20	0.0001
B	65.19	1	65.19	25.17	0.0001
C	15.22	1	15.22	5.88	0.0249
A2	30.44	1	30.44	11.76	0.0027
B2	17.26	1	17.26	6.67	0.0178
Residual	51.79	20	2.59		
Cor. total	236.62	25			

Table 10 The 7-day flexural strength quadratic model with ANOVA analysis

Source	Sum of square	DF	Mean square	*F*-value	*p*-value
Model	4.35	9	0.48	21.79	0.0001
A	2.54	1	2.54	144.22	0.0001
B	0.82	1	0.82	36.98	0.0001
C	0.044	1	0.0044	0.20	0.6634
AB	0.17	1	0.17	7.50	0.0140
AC	0.07	1	0.07	3.22	0.0904
BC	0.01	1	0.01	0.51	0.4837
A2	0.68	1	0.68	30.59	0.0001
B2	0.05	1	0.05	2.43	0.1378
C2	0.01	1	0.01	0.42	0.5279
Residual	0.38	17	0.02		
Cor. total	4.73	26			

Table 11 The 28-day flexural strength quadratic model with ANOVA analysis

Source	Sum of square	DF	Mean square	*F*-value	*p*-value
Model	0.75	3	0.25	13.67	0.0001
A	0.44	1	0.44	23.85	0.0001
B	0.10	1	0.10	5.44	0.0302
B2	0.32	1	0.32	17.75	0.0004
Residual	0.37	20	0.02		
Cor. total	1.11	23			

POFA, the improvement in the mortar's strength subjected to the grinding cycles was not as significant as in SAI.

To further examine the quality of models and the degree of correlation, R^2 was concerned with ensuring a good agreement between experiment data and predicted models. A model with a higher R^2 value that is at least greater than 0.8, closer to 1.0, can be claimed as having fit

Table 12 The 56-day flexural strength 2FI model with ANOVA analysis

Source	Sum of square	DF	Mean square	*F*-value	*p*-value
Model	2.67	5	0.53	10.56	0.0001
A	1.71	1	1.71	33.86	0.0001
B	0.19	1	0.19	3.83	0.0643
C	0.16	1	0.16	3.11	0.0931
AB	0.36	1	0.36	7.05	0.0152
AC	0.25	1	0.25	4.96	0.0375
Residual	1.01	20	0.05		
Cor. total	3.68	25			

Table 13 The 90-day flexural strength 2FI model with ANOVA analysis

Source	Sum of square	DF	Mean square	*F*-value	*p*-value
Model	2.18	3	0.73	19.73	0.0001
A	1.51	1	1.51	40.90	0.0001
B	0.06	1	0.06	1.52	0.2309
AB	0.62	1	0.62	16.79	0.0005
Residual	0.81	22	0.04		
Cor. total	3.00	25			

to the input data and prediction from the model (Adamu et al. 2022, 2021). From the predicted model's statistics presented in Tables 14 and 15, only these 7- and 28-day compressive strength as well as 7-day flexural models had great R^2 which were greater than 0.9. The rest of the prediction model had an R^2 value in the range of 0.67 to 0.82. In addition, the adequate precision of each model was concerned with measuring the signal-to-noise ratio (Waqar et al. 2023). All predicted models have an adequate precision value greater than 4, and thus, they can be used for predicting outcomes with higher accuracy.

All response-coded equations are presented in Eqs. 2, 3, 4, 5, 6, 7, 8 and 9.

$$\text{Compressive strength}_{7\ \text{days}} = 39.82 - 5.25A + 0.48B + 0.72C - 0.59AB - 0.75AC + 0.28BC + 1.43A^2 - 0.68B^2 - 0.33C^2 \quad (2)$$

$$\text{Compressive strength}_{28\ \text{days}} = 50.97 - 5.02A + 1.21B + 0.26C \quad (3)$$

$$\text{Compressive strength}_{56\ \text{days}} = 53.35 - 3.42A + 1.27B \quad (4)$$

$$\text{Compressive strength}_{90\ \text{days}} = 52.38 - 1.90A + 2.10B + 0.76C + 2.77A^2 + 1.59B^2 \quad (5)$$

$$\text{Flexural strength}_{7\ \text{days}} = 8.34 - 0.38A + 0.21B - 0.02C - 0.12AB - 0.08AC - 0.03BC - 0.34A^2 + 0.09B^2 + 0.04C^2 \quad (6)$$

$$\text{Flexural strength}_{28\ \text{days}} = 9.23 - 0.17A + 0.08B + 0.26B^2 \quad (7)$$

$$\text{Flexural strength}_{56\text{days}} = 9.84 - 0.28A + 0.14B - 0.09C - 0.21AB - 0.19AC \quad (8)$$

$$\text{Flexural strength}_{90\ \text{days}} = 10.10 - 0.22A + 0.07B - 0.08C - 0.21AB - 0.06AC - 0.10BC \quad (9)$$

RSM could provide the optimal factors and predicted responses based on the developed model equations and input criteria. From it, users could use the recommended factors for their experiment with an expected response. Thus, each optimizing criterion for having maximum compressive and flexural strength at all curing ages was designed in RSM as presented in Table 16. Among all proposed solutions, the software recommended the optimum factors as follows: 10% micro POFA, 3% nano POFA, and the grinding cycle was

Table 14 Compressive strength using respond surface models' statistics

Responses	7-day compressive strength	28-day compressive strength	56-day compressive strength	90-day compressive strength
R^2	0.96	0.93	0.82	0.82
Adjusted R^2	0.93	0.92	0.80	0.82
Predicted R^2	0.89	0.90	0.76	0.70
Standard deviation	1.20	1.29	1.46	1.49
Mean	40.10	50.97	53.55	55.53
Adequate precision	18.72	26.09	17.79	14.27
Predicted residual error sum of square	59.48	53.38	56.19	71.77

Table 15 Flexural strength using respond surface models' statistics

Responses	7-day compressive strength	28-day compressive strength	56-day compressive strength	90-day compressive strength
R^2	0.92	0.67	0.80	0.82
Adjusted R^2	0.88	0.52	0.75	0.76
Predicted R^2	0.78	0.51	0.66	0.60
Standard deviation	0.15	0.14	0.19	0.13
Mean	8.21	9.41	9.85	10.098
Adequate precision	14.34	12.09	13.98	15.38
Predicted residual error sum of square	1.02	0.55	1.17	0.59

Table 16 Goal criteria for the optimization

Criteria	Optimization target	Lower limit	Upper limit
Micro POFA (%), A	In range	10	30
Nano POFA (%), B	In range	1	3
Grinding cycles, C	In range	50,000	110,000
Compressive strength (MPa) on 7 days	Maximize	45.44	48.837
Compressive strength (MPa) on 28 days	Maximize	56.448	58.628
Compressive strength (MPa) on 56 days	Maximize	57.363	59.504
Compressive strength (MPa) on 90 days	Maximize	58.09	62.651
Flexural strength (MPa) on 7 days	Maximize	7.944	8.9852
Flexural strength (MPa) on 28 days	Maximize	9.103	9.8448
Flexural strength (MPa) on 56 days	Maximize	9.782	10.6092
Flexural strength (MPa) on 90 days	Maximize	10.231	11.06

110,000 where this set solution had the highest desirability value of 0.629. The compressive strength at 7, 28, 56, and 90 days were expected in these values: 48.319, 57.458, 58.336, and 61.497 MPa, while the value of 8.88, 9.727, 10.567, and 10.381 MPa was predicted for 7-, 28-, 56- and 90-day flexural strength. Among the other solutions provided in the software, all solutions recommended the micro POFA replacement at 10%, and the nano POFA's replacement rate was in the range of 2.99 to 3%. However, most solutions with a desirability value above 0.62 suggested using the higher grinding cycles greater than 100 k for a promising result. The optimum mix design was achieved using only 3% of nano POFA, which improved both the compressive and flexural strength of the mortar. The addition of 3% nano POFA may be considered a practical way of enhancing mortar strength as the nano POFA can be prepared using an ordinary LA abrasion machine.

Conclusions

The following conclusion can be drawn from this work:

- Size reduction of POFA using LA abrasion machine successfully produced nano POFA with the size of 103 nm which was obtained at 110k cycles.
- The nano POFA showed a superior pozzolanic reactivity compared to the micro POFA in the SAI test, modified Chapelle test, and TGA test, while all types of POFA were verified as pozzolanic material in the Frattini test. In the SAI test, the 110k nano POFA-based sample had the best performance where it was 25.5% greater than the control sample.
- Increasing the micro POFA replacement in mortar mix from 10 to 30% led to the reduction of workability and hardened strength of mortar, while using a higher dosage of nano POFA up to 3% in the micro POFA-based mortar increased its workability and strength. The grinding cycle of nano POFA had

the least impact on the strength of mortar compared to the composition of micro and nano POFA.
- The results show that nano POFA increased the mortar strength activity index by up to 20% compared to micro POFA.
- The nano POFA provided a 7.45% higher early age strength (7 days) compared to the control sample.
- The optimum mortar mix design was obtained using a combination of 10% micro POFA, and 3% nano POFA, with the highest compressive (62.65 MPa) and flexural (11.06 MPa) strength. The nano POFA with 103 nm has a desirability level of 0.63 which could provide higher hardened strength in mortar.

Abbreviations

LA abrasion machine	Los Angeles abrasion machine
POFA	Palm oil fuel ash
SCM	Supplementary cementitious material
RSM	Response surface modeling
LOI	Loss of ignition
CH	Calcium hydroxide
CSH	Calcium silicate hydrate
ANOVA	Analysis of variance
L	Length
W	Width
H	Height
R^2	Coefficient of determination
p-value	Probability
OPC	Ordinary Portland cement
BET	Brunauer-Emmett-Teller analysis
XRF	X-ray fluorescence
XRD	X-ray diffraction
FESEM	Field emission scanning electron microscope
SAI	Strength activity index
TGA	Thermogravimetric analysis

Acknowledgements
The authors would like to acknowledge the financial support from IIUM-UMPSA Sustainable Research Collaboration Grant (RDU223222), Ministry of Higher Education (FRGS/1/2024/TK05/UMP/01/2), and UMPSA Postgraduate Research Scheme (PGRS220322).

Authors' contributions
YL, methodology, investigation, formal analysis, validation, and writing — original draft preparation. SAS, investigation, methodology, and data curation. NA, data curation and writing — review and editing. KFT, methodology, supervision, funding acquisition, and writing — review and editing. SCC, conceptualization, methodology, investigation, supervision, writing — review and editing, and funding acquisition.

Funding
The work was supported by the IIUM-UMPSA Sustainable Research Collaboration Grant (RDU223222), Ministry of Higher Education (FRGS/1/2024/TK05/UMP/01/2), and UMPSA Postgraduate Research Scheme (PGRS220322).

Availability of data and materials
The datasets used and/or analyzed during the current study are available from the corresponding author on reasonable request.

Declarations

Competing interests
The authors declare that they have no competing interests.

Received: 11 June 2024 Accepted: 20 August 2024
Published online: 29 August 2024

References

Abdalla JA, Thomas BS, Hawileh RA, Yang J, Jindal BB, Ariyachandra E (2022) Influence of nano-TiO2, nano-Fe2O3, nanoclay and nano-CaCO3 on the properties of cement/geopolymer concrete. Cleaner Materials 4:100061. https://doi.org/10.1016/j.clema.2022.100061

Adamu M, Trabanpruek P, Jongvivatsakul P, Likitlersuang S, Iwanami M (2021) Mechanical performance and optimization of high-volume fly ash concrete containing plastic wastes and graphene nanoplatelets using response surface methodology. Constr Build Mater 308:125085. https://doi.org/10.1016/j.conbuildmat.2021.125085

Adamu M, Ibrahim YE, Alanazi H (2022) Evaluating the influence of elevated temperature on compressive strength of date-palm-fiber-reinforced concrete using response surface methodology. Materials 15. https://doi.org/10.3390/ma15228129

American Society for Testing and Materials (ASTM) (2013) ASTM C 618–12a—Standard Specification for Coal Fly Ash and Raw or Calcined Natural Pozzolan for Use in Concrete. American Society for Testing and Materials (ASTM), Philadelphia, PA, USA

Alabduljabbar H, Mohammadhosseini H, Tahir Md, M., Alyousef, R., (2021) Green and sustainable concrete production using carpet fibers waste and palm oil fuel ash. Mater Today Proc 39:929–934. https://doi.org/10.1016/j.matpr.2020.04.047

Al-Kutti W, Nasir M, Johari MAM, Islam ABMS, Manda AA, Blaisi NI (2018) An overview and experimental study on hybrid binders containing date palm ash, fly ash, OPC and activator composites. Constr Build Mater 159:567–577

Alnahhal AM, Alengaram UJ, Yusoff S, Singh R, Radwan MKH, Deboucha W (2021) Synthesis of sustainable lightweight foamed concrete using palm oil fuel ash as a cement replacement material. Journal of Building Engineering 35:102047. https://doi.org/10.1016/j.jobe.2020.102047

Alsubari B, Shafigh P, Ibrahim Z, Jumaat MZ (2018) Heat-treated palm oil fuel ash as an effective supplementary cementitious material originating from agriculture waste. Constr Build Mater 167:44–54. https://doi.org/10.1016/j.conbuildmat.2018.01.134

Altwair NM, Johari MAM, Hashim SFS (2011) Strength activity index and microstructural characteristics of treated palm oil fuel ash. Structure 5

Amran M, Lee YH, Fediuk R, Murali G, Mosaberpanah MA, Ozbakkaloglu T, Yong Lee Y, Vatin N, Klyuev S, Karelia M (2021) Palm oil fuel ash-based eco-friendly concrete composite: a critical review of the long-term properties. Materials 14. https://doi.org/10.3390/ma14227074

Andreão PV, Suleiman AR, Cordeiro GC, Nehdi ML (2020) Beneficiation of sugarcane bagasse ash: pozzolanic activity and leaching behavior. Waste Biomass Valorization 11:4393–4402

Armarego WLF (2022) Chapter 5 - Nanomaterials. In: Armarego WLF (ed) Purification of Laboratory Chemicals (Ninth Edition). Butterworth-Heinemann, pp 586–630. https://doi.org/10.1016/B978-0-323-90968-6.50005-9

Asghar R, Khan MA, Alyousef R, Javed MF, Ali M (2023) Promoting the green construction: scientometric review on the mechanical and structural performance of geopolymer concrete. Constr Build Mater 368:130502. https://doi.org/10.1016/j.conbuildmat.2023.130502

ASTM C (2005) 311–04, "Standard test methods for sampling and testing fly ash or natural pozzolans for use in Portland-cement concrete." Annu B ASTM Stand 4:204–212

Borges AL, Soares SM, Freitas TOG, de Oliveira Júnior A, Ferreira EB, da Ferreira FG, S., (2021) Evaluation of the pozzolanic activity of glass powder in three maximum grain sizes. Mater Res 24:e20200496

Chalee W, Cheewaket T, Jaturapitakkul C (2021) Enhanced durability of concrete with palm oil fuel ash in a marine environment. J Market Res 13:128–137. https://doi.org/10.1016/j.jmrt.2021.04.061

Cheng S, Ge K, Sun T, Shui Z, Chen X, Lu J-X (2021) Pozzolanic activity of mechanochemically and thermally activated coal-series kaolin in cement-based materials. Constr Build Mater 299:123972. https://doi.org/10.1016/j.conbuildmat.2021.123972

Chin SC, Tong FS, Doh SI, Gimbun J, Ong HR, Serigar JP (2018) Strengthening performance of PALF-epoxy composite plate on reinforced concrete beams. In IOP Conference Series: Materials Science and Engineering 318:012026

Chin SC, Moh JNS, Doh SI, Yahaya FM, Gimbun J (2019) Strengthening of reinforced concrete beams using bamboo fiber/epoxy composite plates in flexure. Key Eng Mater 821:465–471

Cho YK, Jung SH, Choi YC (2019) Effects of chemical composition of fly ash on compressive strength of fly ash cement mortar. Constr Build Mater 204:255–264

Cordeiro GC, Andreão PV, Tavares LM (2019) Pozzolanic properties of ultrafine sugar cane bagasse ash produced by controlled burning. Heliyon 5:e02566

EN BS (2005) British Standard Euronorm 196.: methods of testing cement. Part 5: Pozzolanicity test for pozzolanic cement

Fang Y, Tee KF (2017) Structural reliability analysis using response surface method with improved genetic algorithm. Struct Eng Mech 62(2):139–142

Ferraz E, Andrejkovicova S, Hajjaji W, Velosa AL, Silva AS, Rocha F (2015) Pozzolanic activity of metakaolins by the French standard of the modified Chapelle test: a direct methodology. Acta Geodynamica Et Geomaterialia 12:289–298

Hamada H, Tayeh B, Yahaya F, Muthusamy K, Al-Attar A (2020a) Effects of nano-palm oil fuel ash and nano-eggshell powder on concrete. Constr Build Mater 261:119790. https://doi.org/10.1016/j.conbuildmat.2020.119790

Hamada HM, Al-attar AA, Yahaya FM, Muthusamy K, Tayeh BA, Humada AM (2020b) Effect of high-volume ultrafine palm oil fuel ash on the engineering and transport properties of concrete. Case Studies in Construction Materials 12:e00318. https://doi.org/10.1016/j.cscm.2019.e00318

Hamada HM, Al-Attar AA, Tayeh B, Yahaya FBM (2022) Optimizing the concrete strength of lightweight concrete containing nano palm oil fuel ash and palm oil clinker using response surface method. Case Studies in Construction Materials 16:e01061. https://doi.org/10.1016/j.cscm.2022.e01061

Hassan WNFW, Ismail MA, Lee H, Hussin MW, Ismail M, Singh JK (2017) Utilization of nano agricultural waste to improve the workability and early strength of concrete. Int J Sustain Build Technol Urban Dev. 8:316–331. https://doi.org/10.22712/susb.20170030

Hassan WNFW, Ismail M, Ismail MA, Lee HS, Hussin MW (2020) Fresh and hardened properties of high-performance concrete utilising micro and nano palm oil fuel ash. Malays Constr Res J 36

Hossain MM, Karim MR, Elahi MMA, Islam MN, Zain MFM (2020) Long-term durability properties of alkali-activated binders containing slag, fly ash, palm oil fuel ash and rice husk ash. Constr Build Mater 251:119094. https://doi.org/10.1016/j.conbuildmat.2020.119094

Hussin MW, Abdul Shukor Lim NH, Sam ARM, Samadi M, Ismail MA, Ariffin NF, Khalid NHA, Majid MZA, Mirza J, Lateef H (2015) Long term studies on compressive strength of high volume nano palm oil fuel ash mortar mixes. J Teknol 77:15–20. https://doi.org/10.11113/jt.v77.6387

Ibrahim S, Meawad A (2022) Towards green concrete: study the role of waste glass powder on cement/superplasticizer compatibility. Journal of Building Engineering 47:103751. https://doi.org/10.1016/j.jobe.2021.103751

Ismail AH, Kusbiantoro A, Chin SC, Muthusamy K, Islam M, Tee KF (2020) Pozzolanic reactivity and strength activity index of mortar containing palm oil clinker pretreated with hydrochloric acid. J Clean Prod 242:118565

Jaturapitakkul C, Tangpagasit J, Songmue S, Kiattikomol K (2011) Filler effect and pozzolanic reaction of ground palm oil fuel ash. Constr Build Mater 25:4287–4293. https://doi.org/10.1016/j.conbuildmat.2011.04.073

K, S., Das, B.B., (2022) Pozzolanic reactivity and drying shrinkage characteristics of optimized blended cementitious composites comprising of nano-silica particles. Constr Build Mater 316:125796. https://doi.org/10.1016/j.conbuildmat.2021.125796

Kamalakar Mali A, Nanthagopalan P (2021) Development of a framework for the selection of best sugarcane bagasse ash from different sources for use in the cement-based system: a rapid and reliable path. Constr Build Mater 293:123386. https://doi.org/10.1016/j.conbuildmat.2021.123386

Kamalakar MA, Prakash N (2021) Comminution: a supplementation for pozzolanic adaptation of sugarcane bagasse ash. J Mater Civ Eng 33:04021343. https://doi.org/10.1061/(ASCE)MT.1943-5533.0003985

Kim HN, Kim JW, Kim MS, Lee BH, Kim JC (2019) Effects of ball size on the grinding behavior of talc using a high-energy ball mill. Minerals 9. https://doi.org/10.3390/min9110668

Le Tang W (2018) Department of Civil Engineering carbonation of concrete incorporating high volume of micro and low volume of nano palm oil fuel ash

Li B, Yu S, Gao B, Li Y, Wu F, Xia D, Chi Y, Wang S (2023) Effect of recycled aggregate and steel fiber contents on the mechanical properties and sustainability aspects of alkali-activated slag-based concrete. Journal of Building Engineering 66:105939. https://doi.org/10.1016/j.jobe.2023.105939

Lim NHAS, Ismail MA, Lee HS, Hussin MW, Sam ARM, Samadi M (2015) The effects of high volume nano palm oil fuel ash on microstructure properties and hydration temperature of mortar. Constr Build Mater 93:29–34. https://doi.org/10.1016/J.CONBUILDMAT.2015.05.107

Lim JLG, Raman SN, Lai F-C, Zain MFM, Hamid R (2018) Synthesis of nano cementitious additives from agricultural wastes for the production of sustainable concrete. J Clean Prod 171:1150–1160. https://doi.org/10.1016/j.jclepro.2017.09.143

Liu X, Liu L, Lyu K, Li T, Zhao P, Liu R, Zuo J, Fu F, Shah SP (2022a) Enhanced early hydration and mechanical properties of cement-based materials with recycled concrete powder modified by nano-silica. Journal of Building Engineering 50:104175. https://doi.org/10.1016/j.jobe.2022.104175

Liu Y, Tian B, Xiao R, Li Y, Li Z, Cui L, Li Z, Liang H (2022b) The bio-activation of pozzolanic activity of circulating fluidized-bed fly ash by Paenibacilllus mucilaginosus. Adv Powder Technol 33:103621. https://doi.org/10.1016/j.apt.2022.103621

Mali AK, Nanthagopalan P (2021) Development of a framework for the selection of best sugarcane bagasse ash from different sources for use in the cement-based system: a rapid and reliable path. Constr Build Mater 293:123386

Mangi SA, Wan Ibrahim MH, Jamaluddin N, Arshad MF, Shahidan S (2019) Performances of concrete containing coal bottom ash with different fineness as a supplementary cementitious material exposed to seawater. Engineering Science and Technology, an International Journal 22:929–938. https://doi.org/10.1016/j.jestch.2019.01.011

Martins LF, M., Roberto Ribeiro Soares Junior, P., Henrique da Silva, T., de Souza Maciel, P., Peixoto Pinheiro, I., Cesar da Silva Bezerra, A., (2021) Magnesium industry waste and red mud to eco-friendly ternary binder: producing more sustainable cementitious materials. Constr Build Mater 310:125172. https://doi.org/10.1016/j.conbuildmat.2021.125172

Men S, Tangchirapat W, Jaturapitakkul C, Ban CC (2022) Strength, fluid transport and microstructure of high-strength concrete incorporating high-volume ground palm oil fuel ash blended with fly ash and limestone powder. Journal of Building Engineering 56:104714. https://doi.org/10.1016/j.jobe.2022.104714

Mohammad Hosseini H, Ngian SP, Alyousef R, Tahir MM (2021) Synergistic effects of waste plastic food tray as low-cost fibrous materials and palm oil fuel ash on transport properties and drying shrinkage of concrete. Journal of Building Engineering 42:102826. https://doi.org/10.1016/j.jobe.2021.102826

Monteiro H, Moura B, Soares N (2022) Advancements in nano-enabled cement and concrete: innovative properties and environmental implications. Journal of Building Engineering 56:104736. https://doi.org/10.1016/j.jobe.2022.104736

Mostofizadeh S, Tee KF (2021) Static and seismic responses of eco-friendly buried concrete pipes with various dosages of fly ash. Appl Sci 11(24):11700

Muthusamy K, Mirza J, Zamri NA, Hussin MW, Majeed APPA, Kusbiantoro A, Budiea AMA (2019) Properties of high strength palm oil clinker lightweight concrete containing palm oil fuel ash in tropical climate. Constr Build Mater 199:163–177

Norhasri MM, Hamidah MS, Fadzil AM (2017) Applications of using nano material in concrete: a review. Constr Build Mater 133:91–97. https://doi.org/10.1016/j.conbuildmat.2016.12.005

Norhasri MSM, Faiz ARM, Shafienaz I, Shafee HM, Fauzi MAM, Nurliza J (2021) Inclusion of palm oil fuel ash (POFA) as micro engineered material (MEM) in ultra high performance concrete (UHPC). In: Mohd Zuki SS, Mokhatar SN, Shahidan S, Bin Wan Ibrahim MH (eds) Proceedings of the sustainable concrete materials and structures in construction 2020. Springer Singapore, Singapore, pp 57–66

Nur W, Binti F, Hassan W (2019) Mix design optimisation and durability study of high performance concrete containing micro and nano palm oil fuel ash
Oyehan TA, Salami BA, Badmus SO, Saleh TA (2022) Technological trends in activation and modification of palm oil fuel ash for advanced water and wastewater treatment – a review. Sustain Chem Pharm 29:100754. https://doi.org/10.1016/j.scp.2022.100754
Pacewska B, Wilińska I (2020) Usage of supplementary cementitious materials: advantages and limitations. J Therm Anal Calorim 142:371–393. https://doi.org/10.1007/s10973-020-09907-1
Panesar DK, Zhang R (2020) Performance comparison of cement replacing materials in concrete: limestone fillers and supplementary cementing materials – a review. Constr Build Mater 251:118866. https://doi.org/10.1016/j.conbuildmat.2020.118866
Pormmoon P, Abdulmatin A, Charoenwaiyachet C, Tangchirapat W, Jaturapitakkul C (2021) Effect of cut-size particles on the pozzolanic property of bottom ash. J Market Res 10:240–249. https://doi.org/10.1016/j.jmrt.2020.12.017
Raheem AA, Ikotun BD (2020) Incorporation of agricultural residues as partial substitution for cement in concrete and mortar – a review. Journal of Building Engineering 31:101428. https://doi.org/10.1016/j.jobe.2020.101428
Rajak MAA, Majid ZA, Ismail M (2015) Physicochemical characterizations of nano-palm oil fuel ash. p 020018. https://doi.org/10.1063/1.4919156
Rajak MAA, Majid ZA, Ismail M (2019) Pozzolanic activity of nanosized palm oil fuel ash: a comparative assessment with various fineness of palm oil fuel ash. IOP Conf Ser Earth Environ Sci 220:12061. https://doi.org/10.1088/1755-1315/220/1/012061
Rajak MAA, Majid ZA, Ismail M (2021) The effects of nanosized-palm oil fuel ash on early age hydration of hardened cement paste: the microstructure studies. J Adv Res Fluid Mech Therm Sci. 82:87–95. https://doi.org/10.37934/arfmts.82.2.8795
Rajesh Ch, Narasimha Sameer G, Reddy SM, M., Chaitanya Kumar Jagarapu, D., Jogi, P.K., (2020) Consumption of palm oil fuel ash in producing lightweight concrete. Mater Today Proc 33:1073–1078. https://doi.org/10.1016/j.matpr.2020.07.096
Samad AAA, Mohamad N, Ali AZM, Ali N, Goh WI, Hadipramana J, Tee KF (2017) Trends and development of green concrete made from agricultural and construction waste. The Advanced Concrete Technology and Green Materials. ISBN 9789670764979
Samad AAA, Hadipramana J, Mohamad N, Ali AZM, Goh WI, Tee KF (2018) Development of green concrete from agricultural and construction waste. The Transition Towards 100% Renewable Energy. pp 399–410
Samadi M, Huseien GF, Lim NHAS, Mohammadhosseini H, Alyousef R, Mirza J, Rahman ABA (2020) Enhanced performance of nano-palm oil ash-based green mortar against sulphate environment. Journal of Building Engineering 32:101640. https://doi.org/10.1016/j.jobe.2020.101640
Sinsiri T, Kroehong W, Jaturapitakkul C, Chindaprasirt P (2012) Assessing the effect of biomass ashes with different finenesses on the compressive strength of blended cement paste. Mater Des 42:424–433. https://doi.org/10.1016/j.matdes.2012.06.030
Skibsted J, Snellings R (2019) Reactivity of supplementary cementitious materials (SCMs) in cement blends. Cem Concr Res 124:105799
Snehal K, Das BB (2022) Pozzolanic reactivity and drying shrinkage characteristics of optimized blendedcementitious composites comprising of Nano-Silica particles. Construction and Building Materials 316:125796
Sobolev K, Kozhukhova MI, Heintzkill RT (2023) Chapter 3 - Cement-based nano-engineered materials for eco-efficiency. In: Khayat KH, Meng W (eds) Nanotechnology for civil infrastructure. Elsevier, pp 39–68. https://doi.org/10.1016/B978-0-12-817832-4.00002-X
Standard A (2008) ASTM C109-standard test method for compressive strength of hydraulic cement mortars. ASTM International, West Conshohocken, PA
Sun Y, Wang KQ, Lee HS (2021) Prediction of compressive strength development for blended cement mortar considering fly ash fineness and replacement ratio. Constr Build Mater 271:121532. https://doi.org/10.1016/j.conbuildmat.2020.121532
Suraneni P, Hajibabaee A, Ramanathan S, Wang Y, Weiss J (2019) New insights from reactivity testing of supplementary cementitious materials. Cem Concr Compos 103:331–338. https://doi.org/10.1016/j.cemconcomp.2019.05.017
Tabish M, Zaheer MM, Baqi A (2023) Effect of nano-silica on mechanical, microstructural and durability properties of cement-based materials: a review. Journal of Building Engineering 65:105676
Tang WL, Lee HS, Vimonsatit V, Htut T, Singh JK, Hassan WNFW, Ismail MA, Seikh AH, Alharthi N (2019) Optimization of micro and nano palm oil fuel ash to determine the carbonation resistance of the concrete in accelerated condition. Materials 12. https://doi.org/10.3390/ma12010130
Teara A, Doh SI, Chin SC, Ding YJ, Wong J, Jiang XX (2019) Investigation on the durability of use fly ash and eggshells powder to replace the cement in concrete productions. In IOP Conference Series: Earth and Environmental Science 244:012025
Tee KF, Mostofizadeh S (2021) A mini review on properties of Portland cement concrete with geopolymer materials as partial or entire replacement. Infrastructures 6(2):26
Walker R, Pavía S (2011) Physical properties and reactivity of pozzolans, and their influence on the properties of lime–pozzolan pastes. Mater Struct 44:1139–1150
Wan Hassan WNF, Ismail MA, Lee HS, Meddah MS, Singh JK, Hussin MW, Ismail M (2020) Mixture optimization of high-strength blended concrete using central composite design. Constr Build Mater 243:118251. https://doi.org/10.1016/J.CONBUILDMAT.2020.118251
Wang T, Ishida T, Gu R, Luan Y (2021) Experimental investigation of pozzolanic reaction and curing temperature-dependence of low-calcium fly ash in cement system and Ca-Si-Al element distribution of fly ash-blended cement paste. Constr Build Mater 267:121012. https://doi.org/10.1016/j.conbuildmat.2020.121012
Waqar A, Bheel N, Almujibah HR, Benjeddou O, Alwetaishi M, Ahmad M, Sabri MMS (2023) Effect of coir fibre ash (CFA) on the strengths, modulus of elasticity and embodied carbon of concrete using response surface methodology (RSM) and optimization. Results in Engineering 17:100883. https://doi.org/10.1016/j.rineng.2023.100883
Wi K, Lee HS, Lim S, Song H, Hussin MW, Ismail MA (2018) Use of an agricultural by-product, nano sized palm oil fuel ash as a supplementary cementitious material. Constr Build Mater 183:139–149. https://doi.org/10.1016/J.CONBUILDMAT.2018.06.156
Wilińska I, Pacewska B (2018) Influence of selected activating methods on hydration processes of mixtures containing high and very high amount of fly ash. J Therm Anal Calorim 133:823–843. https://doi.org/10.1007/s10973-017-6915-y
Zeyad AM, Megat Johari MA, Tayeh BA, Yusuf MO (2017) Pozzolanic reactivity of ultrafine palm oil fuel ash waste on strength and durability performances of high strength concrete. J Clean Prod 144:511–522. https://doi.org/10.1016/j.jclepro.2016.12.121
Zeyad AM, Tayeh BA, Saba AM, Johari MAM (2018) Workability, setting time and strength of high-strength concrete containing high volume of palm oil fuel ash. The Open Civil Engineering Journal 12:35–46. https://doi.org/10.2174/1874149501812010035
Zeyad AM, Johari MAM, Alharbi YR, Abadel AA, Amran YM, Tayeh BA, Abutaleb A (2021) Influence of steam curing regimes on the properties of ultrafine POFA-based high-strength green concrete. Journal of Building Engineering 38:102204. https://doi.org/10.1016/j.jobe.2021.102204
Zhang H, He B, Zhao B, Monteiro JM, P., (2023) Using diatomite as a partial replacement of cement for improving the performance of recycled aggregate concrete (RAC)-effects and mechanism. Constr Build Mater 385:131518. https://doi.org/10.1016/j.conbuildmat.2023.131518

Publisher's Note